

# A coarse grid extraction of sound signals for computational aeroacoustics

G S Djambazov<sup>1</sup>, C-H Lai<sup>2</sup>, K A Pericleous<sup>3</sup> and Z-K Wang<sup>4</sup>\*

## Abstract

Sound waves are propagating pressure fluctuations, which are typically several orders of magnitude smaller than the pressure variations in the flow field that account for flow acceleration. On the other hand, these fluctuations travel at the speed of sound in the medium, not as a transported fluid quantity. Due to the above two properties, the Reynolds averaged Navier-Stokes (RANS) equations do not resolve the acoustic fluctuations. This paper discusses a defect correction method for this type of multi-scale problems in aeroacoustics. Numerical examples in 1-D and 2-D are used to illustrate the concept.

**Keywords** : Computational aeroacoustics, multi-scale, defect correction methods.

## 1 Introduction

Many problems of fundamental and practical importance are of multi-scale nature. As a typical example, the velocity field in turbulent transport problems fluctuates randomly and contains many scales depending on the Reynolds number of the flow. In another typical example, which is the main concern of this paper, sound waves are several orders of magnitude smaller than the pressure variations in the flow field that account for flow acceleration. These sound waves are manifested as pressure fluctuations of very small magnitude, superimposed on the profile of the time-dependent pressure field and propagated at the speed of sound in the medium. These fluctuations are not transported fluid quantity. As a result, numerical solutions of the Navier-Stokes equations which describe fluid motion do not resolve the small scale pressure fluctuations. On the other hand fluctuations involving very small magnitude will inevitably be swamped by the current floating point computation due to the limitation of the memory as well as the precision of calculation. The finite size of data storage has obviously imposed limitations on the numerical accuracy achieved in solving a given mathematical model, even though it is perfectly correct in the description of the physics. On the other hand, direct numerical simulation to include the above multiple-scale

---

<sup>1</sup> Research fellow. G.Djambazov@gre.ac.uk

<sup>2</sup> Corresponding author. C.H.Lai@gre.ac.uk

<sup>3</sup> K.Pericleus@gre.ac.uk

<sup>4</sup> Research student supported by the University of Greenwich Bursary. Z.K.Wang@gre.ac.uk

\* School of Computing and Mathematical Sciences, University of Greenwich, Old Royal Naval College, Park Row, Greenwich, London SE10 9LS, UK

problems is still an expensive tool for sound analysis [1] based on the existing hardware technology. Therefore one may wish to seek for affordable alternative numerical algorithms.

Established methods for the treatment of elliptic problems, where multi-scale phenomena do not exist, include multilevel method and domain decomposition. Both techniques may be used in conjunction with a parallel computer. One implementation of the latter method is to use it directly on the continuously partial differential equation and the results in various subdomains are then put together using certain techniques. Another implementation concept is to use it on the discretised system. In other words, a global grid is required before the partitioning of the domain. The authors take the first approach of the continuous problem and examine the corresponding coarse grid and fine grid problems taking into account of the multi-scale phenomena in the derivation of the respective models.

In essence, there are at least three different scales embedded in the flow variables, namely (i) the mean flow, (ii) flow perturbations or aerodynamic sources of sound, and (iii) the acoustic perturbation. While flow perturbation or aerodynamic sources of sound may be easier to recover, it is not true for the acoustic perturbation because of its comparatively small magnitude. From an engineering perspective, much of the larger scales behaviour may be resolved with the state-of-the-art CFD packages which implement various numerical methods of solving Navier-Stokes equations. This paper examines, in more detail, a defect correction method, first proposed in [2], and suitably adapted for the derivation of the coarse space mathematical model in order to recover smaller scales that have been left behind. The authors have demonstrated the accurate computation of the time-dependent mean flow and flow perturbations in [3][4][5]. In the present study, a two-scale decomposition of flow variables is considered, i.e. the flow variable  $U$  is written as  $\bar{u} + u$ , where  $\bar{u}$  denotes the mean flow and part of aerodynamic sources of sound and  $u$  denotes the remaining part of the aerodynamic sources of sound and the acoustic perturbation.

This paper follows the basic principle of the defect correction [6] with suitable modification for time dependent problems and applies it to the recovery of the propagating acoustic perturbation. The method relies on the use of a lower order partial differential equation defined on the same computational domain where a residual exists such that the acoustic perturbation may be retrieved through a properly defined coarse mesh.

This paper is organised as follows. First, the derivation of a lower order partial differential equation resulting from the Navier-Stokes equations for the coarse space is given. Truncation errors due to the model reduction are examined. Second, accurate representation of residual on the coarse mesh is discussed. The coarse mesh is designed in such a way as to allow various frequencies of noise to be studied. Suitable interpolation operators are studied for the two different

meshes. Third, numerical tests are performed for different mesh parameters to illustrate the concept. Finally, future work is discussed.

## 2 The defect correction method

The aim here is to solve the non-linear equation

$$\frac{\partial U}{\partial t} + \mathfrak{S}\{U\}U \equiv \frac{\partial(\bar{u} + u)}{\partial t} + \mathfrak{S}\{\bar{u} + u\}(\bar{u} + u) = 0, \quad (1)$$

where  $\mathfrak{S}\{U\}$  is a non-linear operator depending on  $U$ . A concrete example of  $\mathfrak{S}\{U\}$  is given below. For simplicity,  $\mathfrak{S}\{U\}$  is considered to have two different scales of magnitudes as  $\bar{u} + u$ . Note that  $|u| \ll |\bar{u}|$  and that

$$\frac{1}{dt} \int_{t_0}^{t_0+dt} u dt \rightarrow 0,$$

with  $dt$  much larger than any significant period of the perturbation velocity. Here  $t_0$  is certain initial starting time. This integral essentially conveys the message that  $u$  is certain fluctuation and will be damped out over the time interval  $dt$ . The problem here is thus purely related to the scales of magnitude of the dependent variables. In the case of sound generated by the motion of fluid, it is natural to imagine  $\mathfrak{S}\{U\}$  as the Navier-Stokes operator and, therefore,  $\bar{u}$  as the time-dependent mean flow and  $u$  as the acoustic perturbation as described in Section 1. For a 2-D problem,

$$\bar{u} = \begin{bmatrix} \bar{r} \\ \bar{v}_1 \\ \bar{v}_2 \end{bmatrix} \quad u = \begin{bmatrix} r \\ v_1 \\ v_2 \end{bmatrix},$$

where  $r$  is the density of fluid and  $\bar{v}_1$  and  $\bar{v}_2$  are the velocity components along the two spatial axes. Using the summation notation of subscripts, the 2-D Navier-Stokes problem may be written as

$$\begin{aligned} \frac{\partial r}{\partial t} + \frac{\partial(rv_j)}{\partial x_j} &= 0, \\ \frac{\partial v_j}{\partial t} + v_j \frac{\partial v_i}{\partial x_j} + \frac{1}{r} \frac{\partial P}{\partial x_i} - \frac{m}{r} \nabla^2 v_i &= 0, \end{aligned}$$

where  $P$  is the pressure and  $\frac{\mathbf{m}}{\mathbf{r}}\nabla^2 v_i$  is the viscous force along  $i$ -th axis.

Suppose (1) represents the time-dependent Navier-Stokes equations. Expanding  $\frac{\partial(\bar{u} + u)}{\partial t} + \mathfrak{S}\{\bar{u} + u\}(\bar{u} + u)$  and re-arranging the resulting terms, one obtains

$$\frac{\partial \bar{\mathbf{r}}}{\partial t} + \bar{v}_j \frac{\partial \bar{\mathbf{r}}}{\partial x_j} + \bar{\mathbf{r}} \frac{\partial \bar{v}_j}{\partial x_j} + [v_j \frac{\partial(\bar{\mathbf{r}} + \mathbf{r})}{\partial x_j} + \mathbf{r} \frac{\partial(\bar{v}_j + v_j)}{\partial x_j}] = -[\frac{\partial \mathbf{r}}{\partial t} + \bar{v}_j \frac{\partial \mathbf{r}}{\partial x_j} + \bar{\mathbf{r}} \frac{\partial v_j}{\partial x_j}],$$

and

$$\begin{aligned} & \frac{\partial v_i}{\partial t} + \bar{v}_j \frac{\partial v_i}{\partial x_j} + \frac{1}{\bar{\mathbf{r}}} \frac{\partial P}{\partial x_i} - \frac{\mathbf{m}}{\bar{\mathbf{r}}} \nabla^2 v_i \quad (2) \\ & + [\frac{\mathbf{r}}{\bar{\mathbf{r}}} \frac{\partial(\bar{v}_i + v_i)}{\partial t} - (v_j + \frac{\mathbf{r}}{\bar{\mathbf{r}}}(\bar{v}_j + v_j)) \frac{\partial(\bar{v}_i + v_i)}{\partial x_j}] = -[\frac{\partial \bar{v}_i}{\partial t} + \bar{v}_j \frac{\partial \bar{v}_i}{\partial x_j} + \frac{1}{\bar{\mathbf{r}}} \frac{\partial \bar{P}}{\partial x_i} - \frac{\mathbf{m}}{\bar{\mathbf{r}}} \nabla^2 \bar{v}_i]. \end{aligned}$$

It can be seen that (1) may be written as

$$\frac{\partial(\bar{u} + u)}{\partial t} + \mathfrak{S}\{\bar{u} + u\}(\bar{u} + u) \equiv \frac{\partial \bar{u}}{\partial t} + \mathfrak{S}\{\bar{u}\}\bar{u} + \frac{\partial u}{\partial t} + E\{\bar{u}\}u + K[\partial_t, \bar{u}, u] \quad (3)$$

where  $\mathfrak{S}\{\bar{u}\}$  and  $E\{\bar{u}\}$  are operators depending on the knowledge of  $\bar{u}$  and  $K[\partial_t, \bar{u}, u]$  is a functional depending on the knowledge of both  $\bar{u}$  and its derivative and  $u$ . Here

$$E\{\bar{u}\}u = \left[ \begin{array}{c} \frac{\partial \mathbf{r}}{\partial t} + \bar{v}_j \frac{\partial \mathbf{r}}{\partial x_j} + \bar{\mathbf{r}} \frac{\partial v_j}{\partial x_j} \\ \frac{\partial v_i}{\partial t} + \bar{v}_j \frac{\partial v_i}{\partial x_j} + \frac{1}{\bar{\mathbf{r}}} \frac{\partial P}{\partial x_i} - \frac{\mathbf{m}}{\bar{\mathbf{r}}} \nabla^2 v_i \end{array} \right] \quad (4)$$

$$K[\partial_t, \bar{u}, u] = \left[ \begin{array}{c} v_j \frac{\partial(\bar{\mathbf{r}} + \mathbf{r})}{\partial x_j} + \mathbf{r} \frac{\partial(\bar{v}_j + v_j)}{\partial x_j} \\ \frac{\mathbf{r}}{\bar{\mathbf{r}}} \frac{\partial(\bar{v}_i + v_i)}{\partial t} - (v_j + \frac{\mathbf{r}}{\bar{\mathbf{r}}}(\bar{v}_j + v_j)) \frac{\partial(\bar{v}_i + v_i)}{\partial x_j} \end{array} \right] \quad (5)$$

In order to obtain a solution to  $\bar{u}$ , one requires to solve a discretised form of  $\frac{\partial \bar{u}}{\partial t} + \mathfrak{S}\{\bar{u}\}\bar{u} = 0$ . Therefore one may use a CFD analysis package, which effectively solves a discretised form of  $\frac{\partial \bar{u}}{\partial t} + \mathfrak{S}\{\bar{u}\}\bar{u} = 0$  instead of

$\frac{\partial(\bar{u} + u)}{\partial t} + \mathfrak{S}\{\bar{u} + u\}(\bar{u} + u) = 0$ . Following the concept of truncation error in a finite difference method, it is possible to define the truncation error due to the removal of the perturbation part of the flow variable, i.e.

$$\mathbf{t} = \frac{\partial(\bar{u} + u)}{\partial t} + \mathfrak{S}\{\bar{u} + u\}(\bar{u} + u) - \left[ \frac{\partial(\bar{u} + u)}{\partial t} + \mathfrak{S}\{\bar{u}\}(\bar{u} + u) \right]. \quad (6)$$

Using the relation  $\mathfrak{S}\{\bar{u}\}(\bar{u} + u) = \mathfrak{S}\{\bar{u}\}\bar{u} + E\{\bar{u}\}u$ , the truncation error due to the removal of the perturbation part is thus given by

$$\mathbf{t} = K[\partial_t, \bar{u}, u]. \quad (7)$$

Note that this truncation error is not related to the discretisation of a continuous model but is related to the reduction of a more complex continuous mathematical model to a less complex continuous mathematical model. From the knowledge of physics of fluids, the acoustic perturbations  $\mathbf{r}$  and  $v_j$  are of very small magnitude (this is not true for their derivatives), and therefore,  $K$  may be considered negligible due to the reason that any feedback from the propagating waves to the flow may be completely ignored, except in some cases of acoustic resonance, which are not concerned with in this paper. In other words the contribution due to the perturbation part ( $u$ ) has negligible effect on the main background flow ( $\bar{u}$ ) of the fluid. The consequence of this is that one can apply a time-dependent discretisation, as in any CFD analysis packages, to obtain numerical approximations at every time step without considering corrections from the perturbation part at this stage. Such approximations due to a CFD analysis package may be denoted as  $\bar{u}^*$  and their usage is discussed below. The negligible contribution to  $\mathbf{t}$  allows separate computation of the defect at each discretised time step feasible in the present study.

In order that the numerical method may be used for cases of resonance, the concept of a defect has to be applied at every time step. Let  $\bar{u}^{(n)}$  and  $u^{(n)}$  be the approximate solutions at the  $n$ -th time step to (3) and  $\mathbf{d}_t(\cdot, \cdot)$  be the temporal difference operator, which relates the values at both  $n$ -th and  $(n-1)$ -th timestep, includes the temporal truncation error, and is general enough to represent a numerical method in commercial packages. One obtains the semi-discretised form,

$$\begin{aligned} & \mathbf{d}_t((\bar{u} + u)^{(n)}, (\bar{u} + u)^{(n-1)}) + \mathfrak{S}\{(\bar{u} + u)^{(n)}\}(\bar{u} + u)^{(n)} \equiv \\ & \mathbf{d}_t(\bar{u}^{(n)}, \bar{u}^{(n-1)}) + \mathfrak{S}\{\bar{u}^{(n)}\}\bar{u}^{(n)} + \mathbf{d}_t(u^{(n)}, u^{(n-1)}) + E\{\bar{u}^{(n)}\}u^{(n)} + K[\partial_t, \bar{u}^{(n)}, u^{(n)}] \end{aligned} \quad (8)$$

Hence one can evaluate the residue at the  $n$ -th time step of the above expression as

$$\begin{aligned} R^{(n)} &\equiv \mathbf{d}_t((\bar{u} + u)^{(n)}, (\bar{u} + u)^{(n-1)}) + \mathfrak{S}\{(\bar{u} + u)^{(n)}\}(\bar{u} + u)^{(n)} \\ &- [\mathbf{d}_t(\bar{u}^{(n)}, \bar{u}^{(n-1)}) + \mathfrak{S}\{\bar{u}^{(n)}\}\bar{u}^{(n)}] = -[\mathbf{d}_t(\bar{u}^{(n)}, \bar{u}^{(n-1)}) + \mathfrak{S}\{\bar{u}^{(n)}\}\bar{u}^{(n)}], \end{aligned} \quad (9)$$

which may then be substituted into (8) and leads to the  $n$ -th time step correction problem

$$\mathbf{d}_t(u^{(n)}, u^{(n-1)}) + E\{\bar{u}^{(n)}\}u^{(n)} + K[\partial_t, \bar{u}^{(n)}, u^{(n)}] = R^{(n)} \quad (10)$$

As discussed above,  $K[\partial_t, \bar{u}^{(n)}, u^{(n)}]$  is small and can then be neglected. Hence the problem in (10) is a linear problem and may be solved more easily to obtain the acoustics perturbation  $u^{(n)}$ . A non-linear iterative solver is required in order to obtain  $u^{(n)}$  for cases where  $K[\partial_t, \bar{u}^{(n)}, u^{(n)}]$  is not negligible. Hence the equation

$$\mathbf{d}_t(u^{(n)}, u^{(n-1)}) + E\{\bar{u}^{(n)}\}u^{(n)} = R^{(n)},$$

with  $E$  given by (4), which is known as the linearised Euler equation, can be solved with the knowledge of  $\bar{u}^{(n)}$ . The numerics and the techniques involved here are often referred to as Computational AeroAcoustics (CAA) methods.

The remaining question is to obtain an approximate solution  $\bar{u}^{(n)}$  to the original problem (3). It is well known that CFD analysis packages provide excellent methods for the solution of

$$\mathbf{d}_t(\bar{u}^{(n)}, \bar{u}^{(n-1)}) + \mathfrak{S}\{\bar{u}^{(n)}\}\bar{u}^{(n)} = 0.$$

Therefore one requires to use a Reynolds averaged Navier-Stokes package supplemented with turbulence models such as [7, 8] to provide a solution of  $\bar{u}^{(n)}$ . One requires  $\bar{u}^{(n)}$  to be as accurate as possible to capture all the physics of interest from  $(n-1)$ -th to  $n$ -th time step, such as flow turbulence and the presence of vortices. Finally, the approximate solution  $\bar{u}^*$  obtained from the CFD package may be used to compute the residue at the  $n$ -th time step using (9) as  $-[\mathbf{d}_t(\bar{u}^*, \bar{u}^{(n-1)}) + \mathfrak{S}\{\bar{u}^*\}\bar{u}^*]$ .

### 3 Coarse grid sound source computation

In order to simulate accurately the approximate solution,  $\bar{u}$ , to the original problem,

$$\frac{\partial(\bar{u} + u)}{\partial t} + \mathfrak{S}\{\bar{u} + u\}(\bar{u} + u) = 0$$

the QUICK differencing scheme [9] is used which produces sufficiently accurate results of  $\bar{u}$  for the purpose of evaluating the residue as defined in (9). A sufficiently fine mesh has to be used in order to preserve vorticity motion. However, much coarser mesh may be used for the numerical solutions of linearised Euler equations [3, 4, 5]. It certainly has to obey the Courant limit and also to account for the fact that the acoustic wavelength may be larger than a typical flow feature which needs to be resolved, e.g. a travelling vortex [10]. The present defect correction method requires to calculate the residual on the CFD mesh and to transfer these residuals onto the acoustic mesh. Physically, the residual is effectively the sound source that would have disappeared without using the present retrieval technique.

Let  $h$  denote the mesh to be used in the Reynolds averaged Navier-Stokes solver. Instead of evaluating  $\bar{u}^{(n)}$ , one would solve the discretised approximation

$$\mathbf{d}_t(\bar{u}_h^{(n)}, \bar{u}_h^{(n-1)}) + \mathfrak{S}\{\bar{u}_h^{(n)}\}\bar{u}_h^{(n)} = 0$$

to obtain  $\bar{u}_h^*$ . The residue on the fine mesh  $h$  can be computed by using a higher order approximation [5] to  $\mathfrak{S}\{\bar{u}_h^{(n)}\}\bar{u}_h^{(n)}$ . Let  $H$  denote the mesh for the linearised Euler equations solver. Again instead of evaluating  $u$ , one would solve the discretised approximation

$$\mathbf{d}_t(u_H^{(n)}, u_H^{(n-1)}) + E\{\bar{u}_H^{(n)}\}u_H^{(n)} = R_H^{(n)}$$

to obtain  $u_H^{(n)}$ . Here  $R_H^{(n)}$  is the projection of  $R$  onto the mesh  $H$  and  $E_H$  is the discretised approximation of  $E$ . Let  $I_{\{h,H\}}$  be a restriction operator to restrict the residue computed on the fine mesh  $h$  to the coarser mesh  $H$ . The restricted residue can then be used in the numerical solutions of linearised Euler equations. Therefore the two-level numerical scheme is (for non-resonance problems):

```

n := 0;
Do
  n := n + 1;
  Solve  $\mathbf{d}_t(\bar{u}_h^{(n)}, \bar{u}_h^{(n-1)}) + \mathfrak{S}\{\bar{u}_h^{(n)}\}\bar{u}_h^{(n)} = 0$  ;
   $R_H^{(n)} := -I_{\{h,H\}}[\mathbf{d}_t(\bar{u}_h^*, \bar{u}_h^{(n-1)}) + \mathfrak{S}\{\bar{u}_h^*\}\bar{u}_h^*]$  ;
  Solve  $\mathbf{d}_t(u_H^{(n)}, u_H^{(n-1)}) + E\{\bar{u}_H^{(n)}\}u_H^{(n)} = R_H^{(n)}$  ;
   $U_H^{(n)} := \bar{u}_H^{(n)} + u_H^{(n)}$  ; (Corrected result of  $U_H^{(n)}$  is not required on  $h$ .)
Until  $n = n_{\max}$ 

```

Here  $U_H^{(n)}$  denotes the discretised approximation of the resultant solution on mesh  $H$ . Note that  $R_H^{(n)}$  cannot be computed as  $-[I_{\{h,H\}} \mathbf{d}_t(\bar{u}_h^*, \bar{u}_h^{(n-1)}) + \mathfrak{S}\{\bar{u}_h^*\} I_{\{h,H\}} \bar{u}_h^*]$  because  $\mathfrak{S}$  is a non-linear operator. Note also that  $\mathbf{d}_t(u_H^{(n)}, u_H^{(n-1)})$  involves a number of smaller time steps, each of  $\Delta T$ , starting from  $u_H^{(n-1)}$  such that  $u_H^{(n)}$  defines at the same time level as  $\bar{u}^{(n)}$ .

In the actual implementation, a pressure-density relation which also defines the speed of sound  $c$  in air is used:

$$\frac{\partial P}{\partial \mathbf{r}} = c^2 \approx 1.4 \frac{\bar{P}}{\bar{\mathbf{r}}} \quad (11)$$

and the first component of the linearised Euler equations in (4) becomes

$$\frac{\partial P}{\partial t} + \bar{v}_j \frac{\partial P}{\partial x_j} + \bar{\mathbf{r}} c^2 \frac{\partial v_j}{\partial x_j} = -c^2 \left[ \frac{\partial \bar{\mathbf{r}}}{\partial t} + \bar{v}_j \frac{\partial \bar{\mathbf{r}}}{\partial x_j} + \bar{\mathbf{r}} \frac{\partial \bar{v}_j}{\partial x_j} \right] \quad (12)$$

The purpose of this substitution is to make sure that the new fluctuations  $P$  and  $v_i$  do not contain a hydrodynamic component, and hence can be resolved on regular Cartesian meshes [4] which is essential for the accurate representation of the acoustic waves or the fluctuation quantity  $u_H$ . On the other hand, an unstructured mesh may be used to obtain  $\bar{u}_h$ . The two different meshes overlap one another on the computational domain. The computational domain for the linearised Euler equations is not necessarily the same as the one for the CFD solutions. It must be large enough to contain at least the longest wavelength of a particular problem under consideration or a number of wavelengths where propagation is of interest. The numerical example as shown in Section 4 does not contain any complicating solid objects, the restriction operator  $I_{\{h,H\}}$  may then be chosen as an arithmetic averaging process [10].

## 4 Numerical experiments

The propagation of the following one-dimensional pulse is considered: an initial pressure distribution with a peak in the origin generates two opposite acoustic waves in both directions. The exact solution of this problem (13) can be verified by substitution in the linearised Euler equations.

$$\begin{aligned}
P &= f(x - ct) + f(x + ct) \\
\overline{rcv}_1 &= f(x - ct) - f(x + ct) \quad . \\
f(x) &= \begin{cases} \frac{A}{2}(1 + \cos 2\pi x / I), & |x| < I / 2 \\ 0, & |x| \geq I / 2 \end{cases} \quad (12)
\end{aligned}$$

Here  $A$  is the amplitude and  $I$  is the wavelength of the two sound waves that start from the origin ( $x=0$ ) at  $t=0$ . The example was reported in [2]. This paper provides a detailed numerical study on various aspects of the grid parameters being used in the two-level method. The CFD domain is of 12 wavelengths and the CAA domain is of 14 wavelengths.

The effects of the following parameters on the solution accuracy are studied. (a) the ratio  $H:h$ , (b) number of points per wavelength, and (c) the restriction operator for residual transfer from fine grid to coarse grid. In all cases, the norm  $\|P_H - P\|_\infty$  is compared. Here  $P_H$  is the approximation obtained on the coarse mesh (CAA) after correction and  $P$  is the exact solution of the pressure variable by taking  $A = 100$ , which leads to a percentage value of  $\|P_H - P\|_\infty$ .

Let  $\Delta t_h$  and  $\Delta t_H$  be the step lengths in the temporal axis for the CFD mesh and the CAA mesh respectively. Figure 1 shows the effect on the accuracy for Case (a). Here  $\Delta t_h$  and  $\Delta t_H$  are chosen to be 0.000235 and 0.00005875 respectively. Two different mesh sizes for the CFD are chosen and they are 0.05 and 0.025. It can be seen that when  $h$  is not fine enough, say  $h = 0.05$ , to resolve some of the physics, it is still possible to use the mesh  $H = 2h$  or  $H = h$  to recover the small scale signal. If a finer mesh was used, say  $h = 0.025$ , it is possible to use  $H \leq 4h$ . This property essentially links with the Courant number of the coarse mesh for CAA [5], i.e.  $H$ , and is also confirmed in the test performed for Case (b).

Figure 2 shows the effect on the accuracy for Case (b). The most accurate solution may be achieved with more than 12 grid points per wavelength, e.g. 16 or more grid points. This confirms the theoretical study based on Courant limits as discussed in [5]. For number of grid points per wavelength less than 12, the accuracy deteriorates very fast.

Figure 3 shows the effect on the accuracy for Case (c). The restriction operators being used in this test to transfer the function  $g_h$  onto the coarse mesh  $H$  includes

$$\text{3-point formula: } I_{\{h,2h\}} g_h = \frac{1}{4}(g_{i-1} + 2g_i + g_{i+1})$$

$$\text{5-point formula: } I_{\{h,4h\}} g_h = \frac{1}{12} (g_{i-2} + 2g_{i-1} + 6g_i + 2g_{i+1} + g_{i+2})$$

$$\text{7-point formula: } I_{\{h,6h\}} g_h = \frac{1}{16} (g_{i-3} + 2g_{i-2} + 3g_{i-1} + 4g_i + 3g_{i+1} + 2g_{i+2} + g_{i+3})$$

9-point formula:

$$I_{\{h,8h\}} g_h = \frac{1}{48} (g_{i-4} + 2g_{i-3} + 6g_{i-2} + 8g_{i-1} + 14g_i + 8g_{i+1} + 6g_{i+2} + 2g_{i+3} + g_{i+4})$$

For very fine CFD mesh, one can retrieve the small scale signal even on a relatively coarse mesh. In the present study, with  $h = 0.0078125$  one can use  $H \leq 8h$  while still maintaining the accuracy. The accuracy exhibited by using the coarse mesh  $H = 8h = 0.0625$  is compatible with the result for Case (a) as depicted in Figure 1.

## 5 Conclusions

This paper provides a numerical method for the retrieval of sound signals by using defects defined on a coarse space and by obtaining corrections from the coarse space with a lower order partial differential equation. The essential concept here is to decouple the computation into two different scales of magnitude on two different meshes. The derivation of the coarse grid model relies on an expansion of the original partial differential equation for the two scales. One criterion governs the choice of the coarse mesh size is the frequencies range of noise being considered for numerical treatment. Detailed numerical experiments to examine various grid parameters are provided. The truncation error due to solving  $\frac{\partial \bar{u}}{\partial t} + \mathfrak{I}\{\bar{u}\}\bar{u} = 0$  instead of  $\frac{\partial (\bar{u} + u)}{\partial t} + \mathfrak{I}\{\bar{u} + u\}(\bar{u} + u) = 0$  is derived. More realistic examples involving industrial applications are being investigated by the authors and will be reported elsewhere.

## References

1. Avital E.J., Sandham N.D., Luo K.H. Mach wave radiation by time-developing mixing layers Part II: Analysis of the source field. *Theoretical and Computational Fluid Dynamics* 1998; **12**: 73-90.
2. Djambazov G.S., Lai C.-H., Pericleous K.A. A defect correction method for the retrieval of acoustic waves. In: *Domain Decomposition Methods in Sciences and Engineering Vol 12*, Chan et al (eds); DDM.org: Japan, 1999; pp. 289 – 296.
3. Djambazov G.S., Lai C.-H., Pericleous K.A. Development of a domain decomposition method for computational aeroacoustics. In *Domain Decomposition Methods in Sciences and Engineering Vol 9*, Bjorstad et al (eds); DDM.org: Bergen, 1999; pp. 719-725.

4. Djambazov G.S., Lai C.-H., Pericleous K.A. Efficient computation of aerodynamic noise. In Contemporary Mathematics Vol 218, Mandel et al (eds); American Mathematical Society: Philadelphia, 1998; pp. 506-512.
5. Djambazov G.S. Numerical Techniques for Computational Aeroacoustics. PhD thesis, University of Greenwich, London, 1998.
6. Böhmer K., Stetter H.J. Defect Correction Methods: Theory and Applications. Springer Verlag, Heidelberg, 1984.
7. Croft N., Pericleous K.A., Cross M. **PHYSICA**: A multiphysics environment for complex flow processes. In Numerical. Methods for Laminar and Turbulent Flows IX Vol 2, Taylor et al (eds); Pineridge Press, U.K., 1995; pp. 1296.
8. PHOENICS, Version 2.1.3, Cham Ltd, Wimbledon, UK, 1995.
9. Leonard B.P. A stable and accurate convective modelling procedure based on quadratic upstream interpolation. *Computer Methods in Applied Mechanics and Engineering* 1979; **19**: 59-98.
10. Djambazov G.S., Lai C.-H., Pericleous K.A. On the coupling of Navier-Stokes and linearised Euler equations for aeroacoustic simulation. *Computers and Visualisation* 2000, **3**: 9-12

Figure 1: The effect of mesh ratio  $H : h$  on the accuracy.

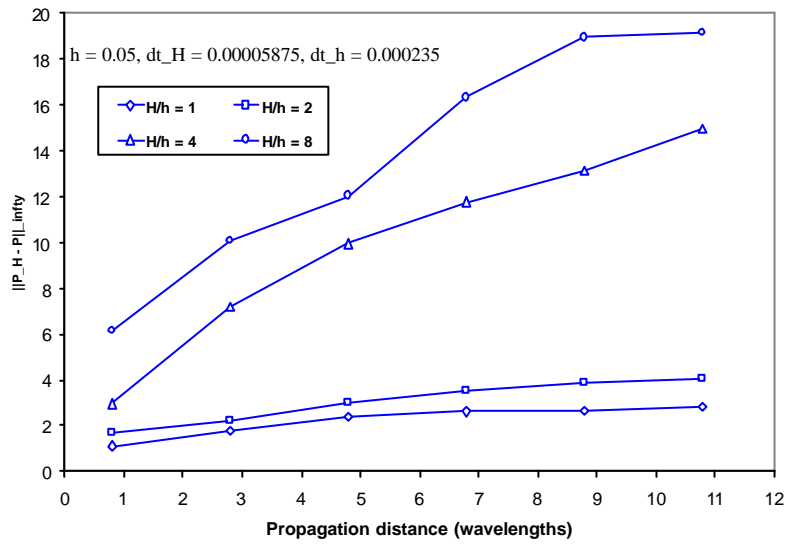
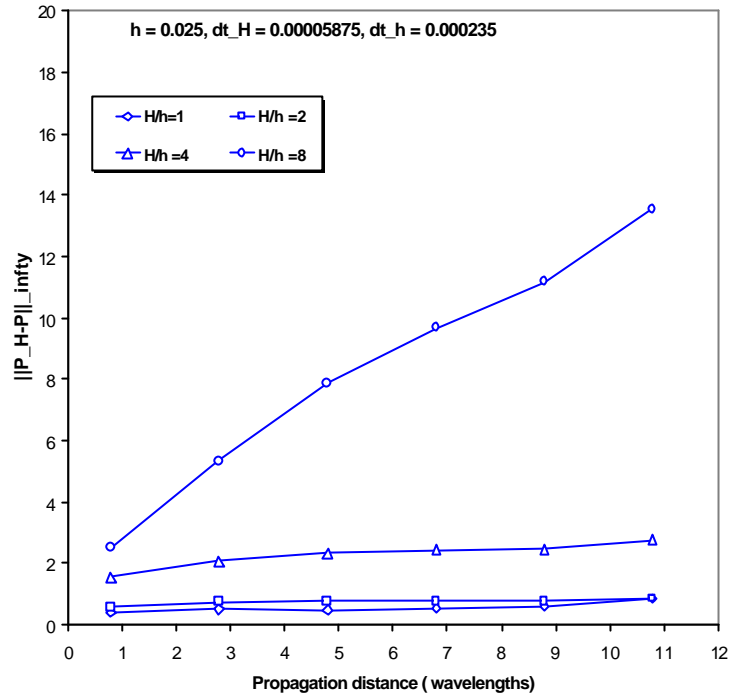


Figure 2: The effect of number of grid points per wavelength on the accuracy.

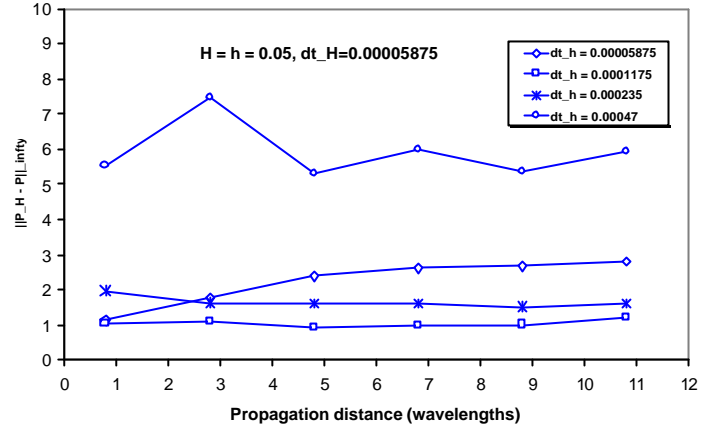


Figure 3: The effect of restriction operators on the accuracy.

